



**HAL**  
open science

## PEM single fuel cell as a dedicated power source for high-inductive superconducting coils

Rafael-Antonio Linares-Lamus, Stéphane Raël, Kévin Berger, Melika Hinaje,  
Jean Lévêque

### ► To cite this version:

Rafael-Antonio Linares-Lamus, Stéphane Raël, Kévin Berger, Melika Hinaje, Jean Lévêque. PEM single fuel cell as a dedicated power source for high-inductive superconducting coils. *International Journal of Hydrogen Energy*, 2018, 43 (11), pp.5913-5921. 10.1016/j.ijhydene.2017.09.013 . hal-01584823

**HAL Id: hal-01584823**

**<https://hal.science/hal-01584823>**

Submitted on 9 Sep 2017

**HAL** is a multi-disciplinary open access archive for the deposit and dissemination of scientific research documents, whether they are published or not. The documents may come from teaching and research institutions in France or abroad, or from public or private research centers.

L'archive ouverte pluridisciplinaire **HAL**, est destinée au dépôt et à la diffusion de documents scientifiques de niveau recherche, publiés ou non, émanant des établissements d'enseignement et de recherche français ou étrangers, des laboratoires publics ou privés.

# PEM single fuel cell as a dedicated power source for high-inductive superconducting coils

Linares Rafael, Raël Stéphane, Berger Kévin, Hinaje Melika\*, Lévêque Jean

Université de Lorraine, – Groupe de Recherche en Electrotechnique et Electronique de Nancy, Faculté des Sciences et Technologies, B.P. 70 239, Vandœuvre-lès-Nancy cedex, 54506, France

Melika.Hinaje@univ-lorraine.fr

**Abstract-** In practice, the voltage of a hydrogen-oxygen fuel cell is around 1 V at open circuit and from 0.6 V to 0.7 V at full rated load and it can be considered as a low-voltage energy source. Moreover, preliminary investigations undertaken on a single proton exchange membrane fuel cell (PEMFC) highlighted its behavior as a DC current source, that can be directly controlled by the H<sub>2</sub> flow rate when the operating point is at very low voltage. In this paper, we present an innovative application of PEMFC that relies on taking advantage of both low voltage level and current source operating mode to feed a high inductive superconducting coil. Such a coil has no resistance and among others, is very sensitive to current ripples. Thus, specific power supplies are designed to feed them but they exhibit in most cases a huge volume and/or a low energy yield. Connecting a superconducting coil to a PEMFC implies to operate in short-circuit, which is an unusual use of PEMFC. To this end, requirements of such an application are defined, by making use of a PEMFC electrical model based on a 1D analog representation of mass transport phenomena. This model, that enables to take into account the influence of gas supply conditions, notably diffusion limit operation, is directly implemented in a standard simulation software used in electrical engineering. Then, simulation results and experimental results obtained by supplying a 10 H superconducting coil cooled by liquid helium by means of a single 100 cm<sup>2</sup> PEMFC are compared and discussed.

**Keywords-** controlled current source; electrochemical dynamic modeling; high-inductive superconducting coil; PEM fuel cell; power supply; short-circuited PEMFC; superconducting coil power supply.

## 1. Introduction

Polymer electrolyte membrane (PEM) fuel cells are by essence low voltage sources. Indeed, the voltage of a single cell is usually near 1 V at open circuit and around 0.6 V at rated conditions of power generation. Thus for power applications, PEMFC composed of several cells connected in series, also called stack, and electronic converters, allowing in particular to rise the voltage to usual application levels are used. Hinaje et al. [1] have led theoretical and experimental investigations in GREEN laboratory (Groupe de Recherche en Electrotechnique et Electronique de Nancy) with a single PEM fuel cell

(PEMFC), either short-circuited or hybridized by discharged supercapacitors, and brought out the electrical behavior as a current source, in which the current is directly controlled by the  $H_2$  flow rate according to Faraday's law (NB: for usual FC applications,  $H_2$  is overfed in comparison to the current generated). The basic principle is schemed in Fig. 1: at very low voltage operation, close to short-circuit conditions, the cell operating point is located in the limit diffusion area that corresponds, in electrical theory, to an ideal current source. This particular behavior of the PEM cell can be of great interest for specific applications requiring a DC current supply under a nearly zero voltage.

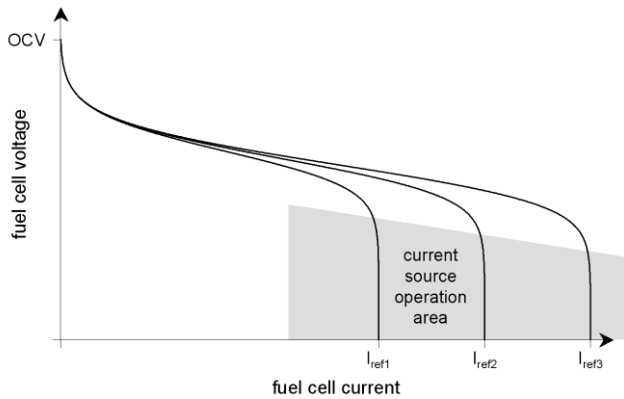


Fig. 1: Representation of the area where FC operates as a current source controlled by  $H_2$  flow rate set by  $I_{ref}$ .

In this paper, we propose an innovative application that takes great advantage of both PEMFC low voltage and current source behavior: the electrical supply for high-inductive superconducting coils. Hinaje et al. [2] have already experimented, in GREEN laboratory, the use of a fuel cell for supplying current to a superconducting coil. However, the experiment was led on a low inductance superconducting coil, i.e. 4 mH, which is not representative of the requirements and problems met with big superconducting coils, as a possible negative voltage across the fuel cell due to a significant value of  $L \times di/dt$ . In this work, a superconducting coil of  $L = 10$  H is supplied by a current,  $I$ , produced by a single FC, what has never been achieved before.

At present, specific electronic power supplies are used to supply superconducting coils and in most of cases they have a huge volume and/or a low energy yield. Indeed, the supply has to respect several constraints such as no current ripples that generate electrical losses in the superconductor material that can cause the accidental loss of the superconductor state, also called quench phenomenon, or even lead to its destruction. Moreover it has to be able to deliver several kA. A disadvantage of such electronic supplies is the generation of harmonic noise onto the industrial grid, and the increase in current to its nominal level has to be achieved carefully. Contrary to those electronic supplies, FCs operating at very low voltages are autonomous (no supply connected to the grid), ensured continuous operation (no risk of power failure due to the grid), together with the electrical quality of the current generated, i.e. free harmonic oscillations. Another advantage not least, to increase the current,

the active area of the electrochemical generator has only to be enhanced, either by connecting single cells in parallel, or by using a single cell with an active area corresponding to the desired current level, whereas high current electronic power supplies lead to heavy, bulky and expensive equipments. Obviously, the proposed solution for the perfectly direct current generation relies upon a PEMFC fed by  $H_2$  from cylinders, for which safety cautions have to be taken. But taking into account the operation of superconducting coils that have to be cooled with liquid nitrogen or helium or by specific cooling, represents by itself a really safety-demanding process, which could easily accommodate the presence of a PEMFC. At last, recent works carried out on a single PEMFC by Bonnet et al. [3] in LRGP laboratory (Laboratoire Réactions et Génie des Procédés) have shown that operating far below the threshold FC voltage (given by the cell manufacturer) does not lead to additional aging in comparison to usual operating conditions.

In the first part, a PEMFC dynamic model based on an analog formulation of transport partial differential equations (PDE), and its implementation in an electrical engineering simulation software (as Saber<sup>®</sup>) are presented. The model details are given in [4]. Then, we demonstrate that this model is suitable to simulate the behaviour of a single PEMFC operating as a controlled current source by means of  $H_2$  flow rate. In the second part, theoretical principles and experimental results of the association of a power superconducting coil and a single FC are presented and discussed. The electrical structure is first described, as well as the experimental bench. Then, simulation investigation and requirements that enable safe FC operation when supplying a huge inductive coil are realized. Finally, the theoretical principles are validated through different experiments led on a  $100\text{ cm}^2$  single PEMFC feeding a 10 H superconducting coil as a load.

## 2. MODEL OF A PEM SINGLE FUEL CELL OPERATING AS A CONTROLLED CURRENT SOURCE

### 2.1 Governing equations

In previous work led by Noiying et al. [4], a PEMFC electrochemical model based on electrical analogy of mass transport phenomena in gas diffusion layers (GDL) and membrane was established. This PDE model is implemented in simulation software commonly used in electrical engineering to design systems (e.g. Saber<sup>®</sup>, in present case). As a result, even if it can be considered of circuit type, and contrary to most circuit models found in the literature such as those presented in [5-10], it naturally includes large signal description, space-dependent parameters in each element of the cell (that is to say local partial pressures in GDL, and water content in the membrane), and also influence of operating conditions (such as FC temperature, gas flow rates, anode and cathode pressures, relative humidity). In this work, our aim is to use it for simulating PEMFC operation as an electrical current source controlled by  $H_2$  flow rate to determine requirements for supplying current to a power superconducting coil.

As presented in Fig. 2, a PEM single cell is composed at each part of the membrane by a catalyst layer (CL) and a GDL [11]. The fuel cell is supplied with hydrogen at anode and oxygen usually from air at cathode, each reactant can be humidified, to either side of a proton exchange membrane coated with platinum-based electrode layers. Protons,  $H^+$ , resulting from hydrogen oxidation pass from the anode to cathode side through the membrane while electrons,  $e^-$ , must flow through an external load, thereby creating electrical current.  $H^+$  then recombine with the electrons and oxygen on the cathode side, forming liquid water as the primary reaction product. The liquid water transport in the membrane is always a balance between at least two competing diffusion mechanisms. One is due to the proton displacement from anode to cathode that drag some water molecules with them, this phenomenon is called electro-osmotic drag. The other mechanism is back diffusion of water from cathode to anode. This water flux results from the water concentration gradient created in the membrane by the electro-osmotic drag and the water produced by the redox reaction at the cathode.

Equations describing gas mixture transport through anode and cathode GDL are reminded hereafter, as well as water transport in the membrane, double layer phenomena, interface and inlets boundary conditions, electrochemical overvoltages at membrane/electrode interfaces, and ohmic voltage drop across the membrane.

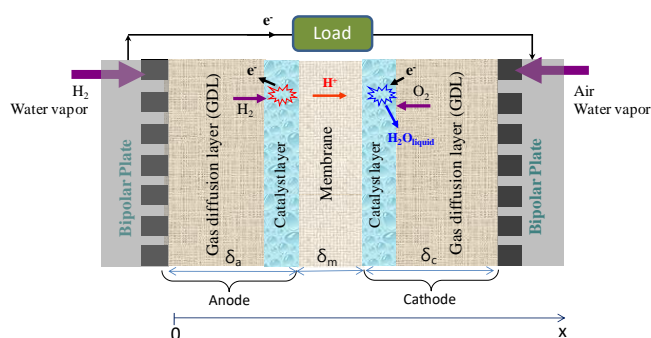


Fig. 2: A single PEMFC's internal structure.

The following assumptions and simplifications in the present model are adopted:

- the cell temperature is homogeneous and constant (indeed the fuel cell is water cooled in the experiment),
- operating conditions are chosen so that gas mixtures are in a single phase (in fact, the fuel cell is fed with 60% RH air at cathode and dry hydrogen at anode) ,
- mass and charge transports are one-dimensional,
- the membrane is homogeneous and gas-tight,
- water exists only in the gas phase at the electrodes, and as solute water in membrane.
- CLs are sufficiently thin to be considered as interfaces.

To describe gas mixture transport in GDLs, both Knudsen and Stefan-Maxwell diffusions are taken into account, so that each gas  $i$  ( $H_2$  or  $H_2O$  at the anode,  $O_2$  or  $N_2$  or  $H_2O$  at the cathode) of the mixture is governed by the following laws:

$$\begin{cases} \frac{\partial P_i}{\partial x} = -\frac{RT}{A_{cell}} \cdot \left( \frac{N_i}{D_{i,eff}} + \sum_{j=1, j \neq i}^e \frac{P_j \cdot N_i - P_i \cdot N_j}{P \cdot D_{ij,eff}} \right) \\ \frac{\partial P_i}{\partial t} = -\frac{RT}{\varepsilon \cdot A_{cell}} \cdot \frac{\partial N_i}{\partial x} \end{cases} \quad (1)$$

where  $e$  is the number of species ( $e_a = 2$  and  $e_c = 3$ ),  $N_i$ ,  $P_i$  and  $D_{i,eff}$  are the molar flow, the partial pressure and the effective Knudsen diffusion coefficient of the gas  $i$ ,  $D_{ij,eff}$  is the effective Stefan-Maxwell diffusion coefficient of gases  $i$  and  $j$ ,  $P$  is the total pressure, and  $\varepsilon$  is the GDL porosity.

The membrane-electrode boundary conditions interfaces ( $x = \delta_a$  and  $x = \delta_a + \delta_m$ ) are linked to reactant consumption, water production, and water molar flow continuity as follow at the anode side:

$$\begin{cases} N_{H_2}(\delta_a) = \frac{I_a}{2F} \\ N_{H_2O_a}(\delta_a) = N_{H_2O_m}(\delta_a) \end{cases} \quad (2)$$

and at the cathode side:

$$\begin{cases} N_{O_2}(\delta_a + \delta_m) = -\frac{I_c}{4F} \\ N_{N_2}(\delta_a + \delta_m) = 0 \\ N_{H_2O_c}(\delta_a + \delta_m) = N_{H_2O_m}(\delta_a + \delta_m) + \frac{I_c}{2F} \end{cases} \quad (3)$$

$I_a$  and  $I_c$  being the Faraday components of anodic and cathodic currents, respectively.

At GDL inlets ( $x = 0$  and  $x = \delta_a + \delta_m + \delta_c$ ), boundary conditions can be written versus gas relative humidities ( $RH_a$ ,  $RH_c$ ), humidifier temperatures ( $T_{hum,a}$ ,  $T_{hum,c}$ ), inlet pressures at the anode and the cathode ( $P_{a,in}$ ,  $P_{c,in}$ ), and gas supply conditions (reference current  $I_{ref}$ , reactant stoichiometries  $\zeta_a$  and  $\zeta_c$ ). It results in the following equations at the anode side:

$$\begin{cases} P_{H_2Oa,in} = RH_a \cdot P_{sat}(T_{hum,a}) \\ P_{H_2,in} = P_{a,in} - P_{H_2Oa,in} \\ N_{H_2,in} = \zeta_a \cdot I_{ref} / (2F) \\ N_{H_2Oa,in} = (P_{H_2Oa,in} / P_{H_2,in}) \cdot J_{H_2,in} \end{cases} \quad (4)$$

and at the cathode side:

$$\begin{cases} P_{H_2Oc,in} = RH_c \cdot P_{sat}(T_{hum,c}) \\ P_{O_2,in} = 0.21 \cdot (P_{c,in} - P_{H_2Oc,in}) \\ P_{N_2,in} = 0.79 \cdot (P_{c,in} - P_{H_2Oc,in}) \\ N_{O_2,in} = -\zeta_c \cdot I_{ref} / (4F) \\ N_{H_2Oc,in} = (P_{H_2Oc,in} / P_{O_2,in}) \cdot N_{O_2,in} \\ N_{N_2,in} = (P_{N_2,in} / P_{O_2,in}) \cdot N_{O_2,in} \end{cases} \quad (5)$$

Water transport in the membrane is due to both diffusion and electro-osmotic drag. Then, it can be expressed that way:

$$\begin{cases} N_{H_2Om} = \frac{n_d}{F} \cdot I_m - A_{cell} \cdot D_{H_2Om} \cdot \frac{\partial c_{H_2O}}{\partial x} \\ \frac{\partial c_{H_2O}}{\partial t} = -\frac{1}{A_{cell}} \cdot \frac{\partial N_{H_2Om}}{\partial x} \end{cases} \quad (6)$$

where  $N_{H_2Om}$  is the water molar flux,  $c_{H_2O}$  is the water concentration,  $I_m$  is the membrane ionic current,  $n_d$  is the electro-osmotic drag coefficient (defined as the number of water molecules dragged per proton), and  $D_{H_2Om}$  is the water diffusion coefficient.

Taking into account, at the membrane-electrode interfaces, the continuity of water molar flow ( $x = \delta_a$  and  $x = \delta_a + \delta_m$ ) and the water phase change (vapour phase in GDLs, liquid phase in the membrane) using of sorption curves, membrane water content  $\lambda$  at membrane boundaries is computed versus water activity  $a = P_{H_2O} / P_{sat}$  as:

$$\begin{cases} \lambda(\delta_a) = \lambda_{sorp} \left( \frac{P_{H_2Oa}(\delta_a)}{P_{sat}(T_{cell})} \right) \\ \lambda(\delta_a + \delta_m) = \lambda_{sorp} \left( \frac{P_{H_2Oc}(\delta_a + \delta_m)}{P_{sat}(T_{cell})} \right) \end{cases} \quad (7)$$

$\lambda$  is defined versus the membrane proton exchange capacity  $X_m$  that corresponds to the number of available sulfonic sites per mass unit, membrane density  $\rho_m$  and water concentration by:

$$\lambda = \frac{c_{H_2O}}{X_m \cdot \rho_m} \quad (8)$$

The required parameters of the model are available in [4].

Using an electrical analogy, pressures and water content can be assimilated to voltages, and molar flux to electric currents. Then water transport in the membrane is computed by space discretization of PDE (1) and (6). It results in the model structure depicted in Fig. 3 which is implemented in Saber® software. It consists in two parts coupled to each other.

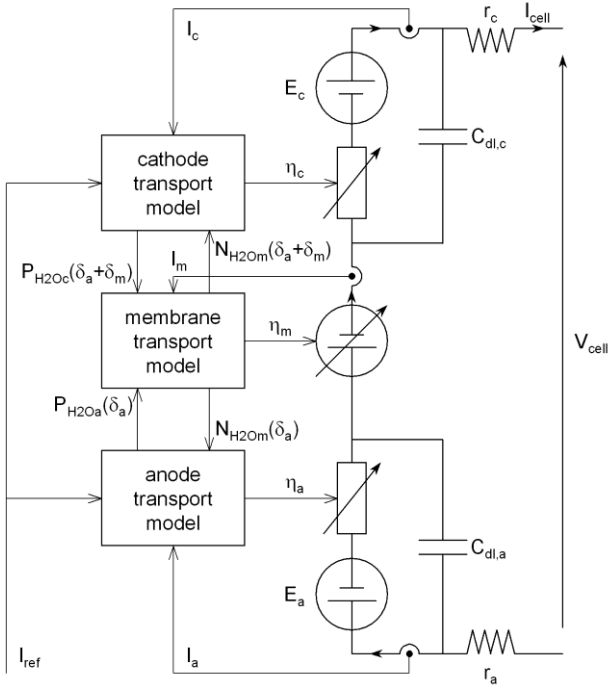


Fig. 3: PEMFC model implemented in electrical engineering simulation software [4].

The first part is dedicated to mass transport and associated variables: gas flows and partial pressures in GDL, water content and water flow in the membrane. Then, electrochemical overvoltages at the membrane/electrode interfaces are calculated by means of Butler-Volmer equation, and the membrane voltage drop is deduced from its non-linear ionic resistance (which locally depends on membrane water content).

The second part is a standard electrical circuit including double layer capacitors and electronic resistances of both electrodes, in addition to electrochemical interfaces and the membrane. This electrical part of the model computes the FC voltage as a function of FC current, equilibrium potentials, overvoltages (note that these are non ideal voltage sources, thus they can be connected in parallel with double layer capacitors without any resolution trouble), and membrane voltage drop. Analog formulations of PDE (1) and (6), their implementations in Saber® software, and computation of all overvoltages are described in more details in [4].

## 2.2 Simulation of PEMFC low voltage operation

Fig. 4 shows the FC current of a short-circuited PEMFC. The dashed line is an experimental curve, recorded with a 100 cm<sup>2</sup> single cell supplied by air and pure dry H<sub>2</sub>. The FC temperature is kept at 60 °C, by a water cooling system. Air relative humidity is set approximately at 60 % by means of a bubble humidifier. Inlet gas pressures are the ambient level and their flow rates are set by a reference current  $I_{ref}$ , as follows:

$$\begin{cases} d_{H_2} = \frac{I_{ref}}{2F} \cdot \frac{RT_0}{P_0} \cdot \zeta_a \cdot 1000 \cdot 60 \\ d_{air} = \frac{I_{ref}}{4F} \cdot \frac{RT_0}{P_0} \cdot \frac{1}{0.21} \cdot \zeta_c \cdot 1000 \cdot 60 \end{cases} \quad [\text{L min}^{-1}] \quad (9)$$

where  $T_0 = 273 \text{ K}$ ,  $P_0 = \text{Pa}$ ,  $\zeta_a$  and  $\zeta_c$  are anode and cathode over-stoichiometric coefficients, respectively. As it can be seen on the experimental short-circuit current, the steady state current value is 20 A, from which the H<sub>2</sub> flow rate could be so at the anode inlet. It can also be noticed that the FC current first rises strongly, and remains higher than the setpoint current,  $I_{ref} = 20 \text{ A}$ , during several tens of seconds. This transient current overshoot corresponds to the H<sub>2</sub> stored in the inlet pipe and in GDL during the initial zero current operation that occurs before applying short-circuit.

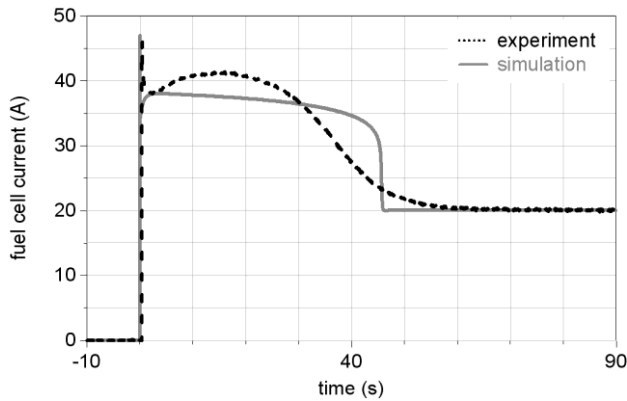


Fig. 4: Experimental (dashed line) and simulated (solid line) fuel cell short-circuit current. Gas flow setting:  $I_{ref} = 20 \text{ A}$ ,  $\zeta_a = 1$ ,  $\zeta_c = 4$

In Fig. 4, the current response obtained with the model is plotted in solid line. Using electrical analogy, the anode inlet pipe volume can be represented by means of an input capacitor. As it can be seen in the computed short-circuit current, the model describes correctly the overall experimental result, that is to say the current source operation in steady-state, and transient current overshoot. Both are of major importance to determine the correct H<sub>2</sub> flow rate slope, when using a FC as a controlled

current source to supply a huge inductance. Even if the results are qualitatively validated, some inaccuracies can be observed during transient, they mainly come from the 1D approximation of reactant transport and redox reactions. Indeed, a 3D model is required for better quantitative results [12-14].

### 3. SINGLE PEMFC FEEDING A 10 H SUPERCONDUCTING COIL: PRINCIPLES AND EXPERIMENTAL RESULTS

#### 3.1 Structure of the superconducting coil current supplied by a PEMFC

The electrical structure is presented in Fig. 5. It is composed of a 100 cm<sup>2</sup> single PEMFC fed by pure H<sub>2</sub> and air, a high current MOS transistor for emergency stop, a superconducting coil with its protection resistor, and a free-wheeling diode (FWD) to ensure current continuity in the inductive coil.

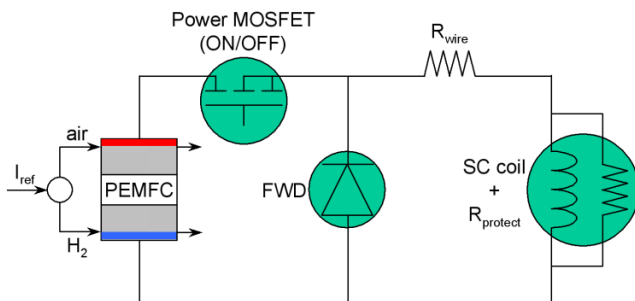


Fig. 5: Electrical scheme of the superconducting coil current supply

The single fuel cell is water cooled in order to regulate its temperature at 60 °C, air relative humidity is approximately 75 % and anode and cathode pressures are 1 atm. To ensure the PEMFC operation as a controlled current source over a large current range, the total circuit resistance (load, wire and contact resistance) must be as low as possible. To this end, the power switch, a 100 V – 1200 A MOSFET, has been selected according to this criterion. Indeed, its on-state resistance is about 1 mΩ when its gate is biased by a 15 V voltage source. It results in a total resistance of the loop close to 2 mΩ, which includes the switch and the wires connecting the switch to the FC. To be in superconducting state (no resistance), the 10 H coil is cooled by liquid helium and is protected by a 0.7 Ω resistor (1 Ω at ambient temperature). The total resistance of connections between the coil and the fuel cell is about 10 mΩ. Fig. 6 present a picture of the experimental test bench. On the left, a picture of the superconducting coil is presented before putting it in the cryostat. The whole fuel cell system including its auxiliaries (humidifier, flow controllers, cooling system, emergency switch...) and the acquisition system are shown on the right picture.

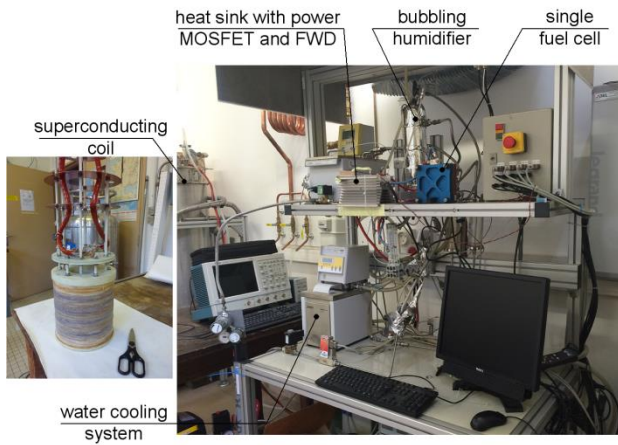


Fig. 6: Experimental test bench composed of FC system (right) and superconducting coil outside the cryostat (left).

### 3.2 Coil current setpoint by the $H_2$ flow rate

Fig. 7 hereafter presents the coil current waveform (i.e. the current through the parallel association of the superconducting inductor and its protection resistor) and the FC voltage when simulating the coil supply by means of the FC, by turning-on the power switch. The FC is initially fed with gases, with the following setpoint:  $I_{ref} = 20$  A,  $\zeta_a = 1$ ,  $\zeta_c = 4$ . As it can be noticed, the coil current is regulated in steady-state to the corresponding  $H_2$  flow rate setpoint. Whereas in transient, the FC current source operation cannot be controlled due to the  $H_2$  previously stored in the anode pipe and it results in a current overshoot, then to a FC operation at negative voltage induced by the coil when the current decreases to reach its steady state level. It can be observed here that the negative voltage applied to the FC during this phase is limited by the FWD on-state voltage drop, to approximately -0.7 V in case of a PN diode use, or to -0.4 V in the case of Schottky diode use.

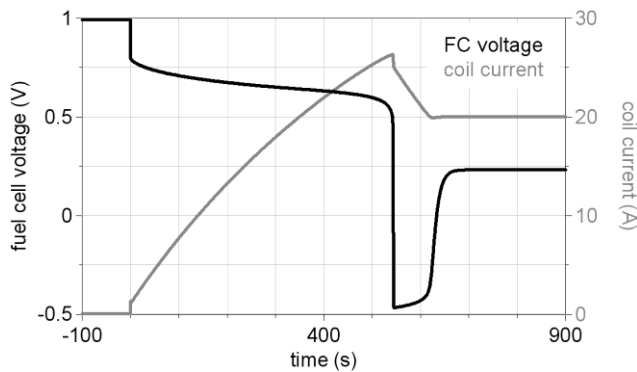


Fig. 7: Simulated coil current and FC voltage at switch turn-on. Gas flow setting:  $I_{ref} = 20$  A,  $\zeta_a = 1$ ,  $\zeta_c = 4$ . FC supplied with gases before turn-on.

To avoid this kind of operation that might imply early aging of the PEMFC, the circuit has to be closed before supplying the FC with gases. The second requirement to avoid FC negative voltage operation, is to limit the slope of  $H_2$  flow rate variation, in order to remain in the area where the FC operates as a controlled current source.

To depict this requirement, Fig. 8a presents the simulation results of the superconducting coil current and the fuel cell voltage when a step of gas flow rates are applied, from  $I_{ref} = 25$  A up to  $I_{ref} = 30$  A (over-stoichiometry:  $\zeta_a = 1$ ,  $\zeta_c = 4$ ). Initially, the single cell is operating in the current source mode, at 25 A. During current increase, as  $H_2$  flow rate is higher than the demanded actual level of current, the FC is overfed, so that it operates in normal mode. This leads to a current overshoot, followed by a regime at negative voltage, as in the case presented in Fig. 7.

On the contrary, when  $H_2$  flow rate is slowly increased, the FC remains in current source mode (Fig. 8b), which means that the current increase is controlled through  $H_2$  flow rate. To get such a dynamic control, the  $H_2$  flow rate variation, i.e.  $dI_{ref}/dt$ , has to be small enough in order that the corresponding transient inductance voltage, i.e.  $L \times dI_{ref}/dt$ , which is added to the circuit resistance voltage drops, has a level compatible with the FC operating as a current source.

For instance, let us consider an increase in coil current from 25 A up to 35 A (corresponding to the experimental test presented in section 3.3). The steady state at 35 A results in a FC voltage equal to about 350 mV (i.e.  $10 \text{ m}\Omega \times 35 \text{ A}$ ). If the increase is linearly operated within 1000 s that matches to a transient inductance voltage of about 100 mV (i.e.  $10 \text{ H} \times 10 \text{ mA s}^{-1}$ ), the FC voltage is lower than 450 mV throughout the current increase duration. Such low voltage level at a current density less or equal to  $0.35 \text{ A.cm}^{-2}$  ensures the PEMFC to operate as a current source controlled by means of  $H_2$  flow rate.

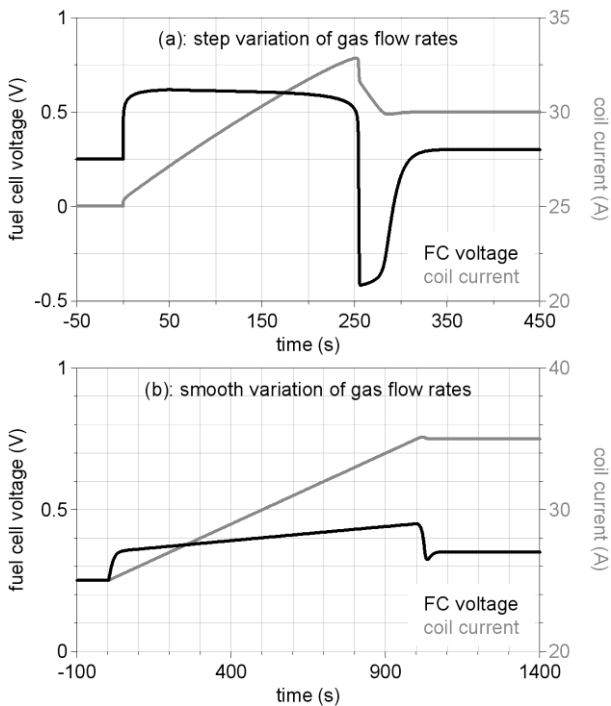


Fig. 8: Simulated coil current and FC voltage for a transition of gas flow rates. Initial gas flow setting:  $I_{ref} = 25$  A,  $\zeta_a = 1$ ,  $\zeta_c = 4$ . (a): Step variation of gas flow rates. Step amplitude:  $\Delta I_{ref} = 5$  A. (b): Smooth variation of gas flow rates. Gas flow variation:  $\Delta I_{ref} = 10$  A,  $dI_{ref}/dt = 10$  mA s<sup>-1</sup>.

To illustrate this example, Fig. 8b presents the coil current and the FC voltage when computing a linear increase of gas flow rates, from  $I_{ref} = 25$  A to  $I_{ref} = 35$  A during 1000 s (over-stoichiometry:  $\zeta_a = 1$ ,  $\zeta_c = 4$ ). As previously in Fig. 8a, the PEMFC is initially operating as a current source supplying 25 A. It can be noticed that the coil current increases from 25 A up to 35 A at the expected rate, i.e. 10 mA.s<sup>-1</sup>. Almost no current overshoot is observed, and the FC voltage remains positive all over the transient.

### 3.3 Experimental results

Fig. 9 shows the experimental coil current and the FC voltage measured in the same conditions as in the simulation associated to Fig. 7 (i.e. at switch turn-on, the cell being initially fed with gases, with the following setting:  $I_{ref} = 20$  A,  $\zeta_a = 1$ ,  $\zeta_c = 4$ ). As previously for the simulation results, it can be noticed that in steady-state, the coil current is regulated at 20 A by means of H<sub>2</sub> flow rate, and that the transient response gives rise to a current excess, and to a FC operation at negative voltage when the current falls to its steady-state level.

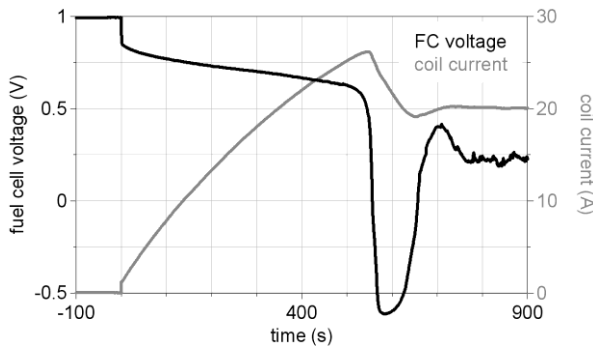


Fig. 9: Experimental coil current and FC voltage at switch turn-on. Gas flow setting:  $I_{ref} = 20$  A,  $\zeta_a = 1$ ,  $\zeta_c = 4$ . Fuel cell supplied with gases before turn-on.

Fig. 10a (experiment) hereafter is comparable to Fig. 8a (simulation). It presents the experimental superconducting coil current and the single cell voltage when rising suddenly gas flow rates from  $I_{ref} = 25$  A up to  $I_{ref} = 30$  A (over-stoichiometry:  $\zeta_a = 1$ ,  $\zeta_c = 4$ ), the PEMFC being initially in current source operating mode, at 25 A. The same conclusions, as the ones that have been deduced from simulation results depicted in Fig. 8a, can be made: during transient, , the FC is overfed and operates

in normal mode, which induces a current overshoot, followed by a negative voltage operation for the FC. To avoid such phenomena, the slope of H<sub>2</sub> flow rate variation has to be limited, in order to control the current increase.

Such a possible control by H<sub>2</sub> flow rate in transient is highlighted in Fig. 10b and Fig. 11. The first figure presents experimental results as a linear increasing transition of 10 mA.s<sup>-1</sup> slope of gas flow rates is applied from  $I_{ref} = 25$  A up to  $I_{ref} = 35$  A (as in Fig. 8b). As computed, the superconducting coil current increases following the expected slope, thus it is actually controlled by the FC, through the H<sub>2</sub> flow rate. As a result, nearly no current overshoot is observed, and the FC voltage remains positive during the transient.

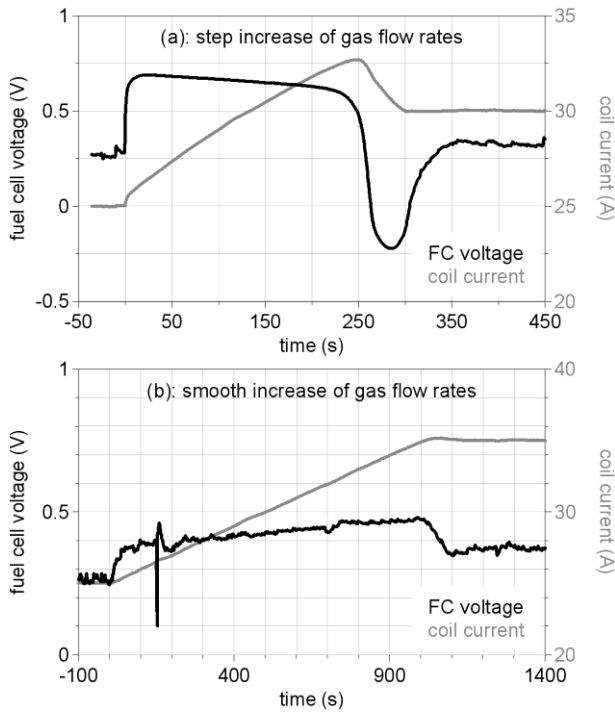


Fig. 10: Experimental coil current and FC voltage for a transition of gas flow rates. Initial gas flow setting:  $I_{ref} = 25$  A,  $\zeta_a = 1$ ,  $\zeta_c = 4$ . (a): Step variation of gas flow rates. Step amplitude:  $\Delta I_{ref} = 5$  A. (b): Smooth increase of gas flow rates. Gas flow variation:  $\Delta I_{ref} = 10$  A,  $dI_{ref}/dt = 10$  mA s<sup>-1</sup>.

Fig. 11 also shows possible effective current control by H<sub>2</sub> flow rate, but in this case during current decrease. During this current decline, the transient inductance voltage induced by the variation of H<sub>2</sub> flow rate, i.e.  $L \times dI_{ref}/dt$ , is negative and may lead to a negative voltage operation of the FC. It can be easily avoided by setting the H<sub>2</sub> flow rate slope at a value for which the inductive term  $L \times dI_{ref}/dt$  does not entirely compensate the circuit resistance voltage drops. In the example of Fig. 11, where experimental results of a decreasing linear transition of gas flow rates from  $I_{ref} = 35$  A down to  $I_{ref} = 25$  A, the current slope limit is equal to  $-25$  mA s<sup>-1</sup> (i.e.  $-10$  m $\Omega \times 25$  A / 10H). As the experiment was led with a slope of  $-20$  mA s<sup>-1</sup>, it can be noticed

in Fig. 11 that the FC effectively runs as a current source, with a positive voltage all over the transient.

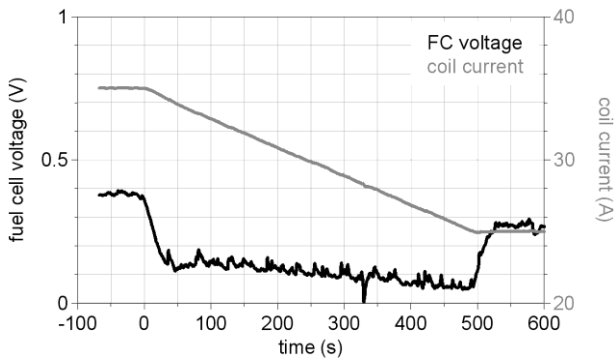


Fig. 11: “Experimental coil current and FC voltage for a slow decrease of gas flow rate. Initial gas flow setting:  $I_{ref} = 35$  A,  $\zeta_a = 1$ ,  $\zeta_a = 4$ . Gas flow variation:  $\Delta I_{ref} = -10$  A,  $dI_{ref}/dt = -20$  mA s<sup>-1</sup>.”

#### 4. CONCLUSION

In this paper, an original and innovating application of FC used as controlled current source has been highlighted, by supplying a huge inductive superconducting coil of 10H. This new application has been firstly simulated by means of a dynamic large signal model in order to determine requirements, that is to say an efficient control of time current variation by means of H<sub>2</sub> flow rate to prevent from current overshoot avoiding that way FC negative voltage. The simulation results have been then validated by means of experiments led on a 100 cm<sup>2</sup> PEMFC supplying a 10 H superconducting coil cooled by liquid helium. To our state of knowledge, the application depicted above is totally novel since no literature sources, describing the use of FC operating as a current source controlled by H<sub>2</sub> flow rate for supplying energy to power superconducting coils, can be found. This particular operation needs the fuel cell to run in short-circuit, which is a totally unusual application for fuel cells. Moreover, such an application is of a great interest since it provides an electric current in essence ready for use, i.e. responding to superconducting device constraints: direct current, generated at very low voltage, free of detrimental harmonics or ripples, independent from the grid that is to say not subject to grid power failures. High current level can be simply reached in theory, by connecting single FC cells in parallel, or by increasing its active area. To this end, further works have to be carried out to assess the feasibility of these techniques at high current level: controlling current by H<sub>2</sub> flow rate when paralleling several single FCs, investigating current density distribution when operating a large (several hundreds of cm<sup>2</sup>) single FC as a current source.

#### ACKNOWLEDGEMENTS

We would like to acknowledge the cryogenic centre of the IJL institute (Institut Jean Lamour), and more especially Thomas Hauet for allowing us to carry out these experiments in the research centre, and Luc Moreau for his help during experimental

tests.

## NOMENCLATURE

$a$  : Water activity (-)

$A$  : Active surface ( $\text{m}^2$ )

$c$  : Concentration ( $\text{mol m}^{-3}$ )

$C$  : Capacitor (F)

$D$  : Diffusion coefficient of species ( $\text{m}^2 \text{s}^{-1}$ )

$E$  : Equilibrium potential (V)

$F$  : Faraday's constant, 96472 ( $\text{C mol}^{-1}$ )

$I$  : Current (A)

$j_0$  : Exchange current density ( $\text{A m}^{-2}$ )

$N$  : Molar flow ( $\text{mol.s}^{-1}$ )

$nd$  : Electro-osmotic drag coefficient (-)

$P$  : Pressure (Pa)

$R$  : Gas constant, 8.314 ( $\text{J mol}^{-1} \text{K}^{-1}$ )

$RH$  : Relative humidity (-)

$t$  : Time (s)

$T$  : Temperature (K)

$V$  : Voltage (V)

$x$  : 1D coordinate (m)

$X$  : Proton exchange capacity ( $\text{mol kg}^{-1}$ )

### Greek letters

$\alpha$  : Transfer coefficient (-)

$\delta$  : Layer thickness (m)

$\varepsilon$  : Porosity (-)

$\varphi$  : Electrical potential (V)

$\eta$  : Surface overvoltage (V)

$\lambda$  : Membrane water content (-)

$\zeta$  : Stoichiometry coefficient (-)

$\rho$  : Density (kg.m<sup>-3</sup>)

$\sigma$  : Electrical conductivity (S m<sup>-1</sup>)

#### Subscripts

a : Anode

c : Cathode

cell : Fuel cell

dl : Double layer

eff : Effective value

hum : Humidifier

in : Inlet

i, j : Species (H<sub>2</sub>, O<sub>2</sub>, H<sub>2</sub>O, N<sub>2</sub>)

m : Membrane

ref : Reference condition

s : Electronic phase

sat : Saturated value

sorp : Sorption

#### REFERENCES

- [1] Hinaje M., Raël S., Caron J.-P., Davat B., An innovating application of PEM fuel cell: current source controlled by hydrogen supply, *International Journal of Hydrogen Energy*, September 2012, 37(174): 12481-12488.
- [2] Hinaje M., Berger K., Lévêque J., Davat B., Superconducting coil fed by PEM fuel cell, *International Journal of Hydrogen Energy*, May 2013, 38 (16): 6773-6779.
- [3] Bonnet C., Lopicque F., Belhadj M., Gerardin K., Raël S., Hinaje M., Mitchell L., Goldsmith V., Kmiotek S. J., Can PEM fuel cells experience appreciable degradation at short circuit ?, *Fuel Cell*, June 2016, 17 (2): 157-165.
- [4] Noiying P., Hinaje M., Thounthong P., Raël S., Davat B., Using electrical analogy to describe mass and charge transport in PEM fuel cell, *Renewable Energy*, 44, 128-140, (2012).
- [5] Yu D., Yuvarajan S., Electronic circuit model for proton exchange membrane fuel cells, *Journal of Power Sources*, March 2005, 142: 238-242.

- [6] Andujar J. M., Segura F., Vasallo M. J., A suitable model plant for control of the set fuel cell DC/DC converter, *Renewable Energy*, April 2008, 33: 813-826.
- [7] Lazarou S., Pyrgioti E., Alexandridis A. T., A simple electric circuit model for proton exchange membrane fuel cells, *Journal of Power Sources*, May 2009, 190 (2): 380-386.
- [8] Chiu L. Y., Diong B., Gemmen R. S., An improved small-signal model of the dynamic behaviour of PEM fuel cells, *IEEE Transactions on Industry Applications*, July 2004, 40 (4): 970-977.
- [9] Page S. C., Anbuky A. H., Krumdieck S. P., Brouwer J., Test method and equivalent circuit modeling of a PEM fuel cell in a passive state, August 2007, *IEEE Transactions on Energy Conversion*, 22 (3): 764-773.
- [10] Fontès G., Turpin C., Astier S., A large signal and dynamic circuit model of a H<sub>2</sub>/O<sub>2</sub> PEM fuel cell: description, parameter identification and exploitation, *IEEE Transactions on Industrial Electronics*, June 2010, 57 (6): 1874-1881.
- [11] Hinaje M., Nguyen D. A., Raël S., Davat B., Bonnet C., Lopicque F., 2D modelling of a defective PEMFC, *International Journal of Hydrogen Energy*, August 2011, 36 (17): 10884-10890.
- [12] Macedo-Valencia J., Sierra J.M., Figuerola-Ramírez S.J., Díaz S.E., Meza M., 3D CFD modeling of a PEM fuel cell stack, *International Journal of Hydrogen Energy*, December 2016, 41 (48): 23425-23433.
- [13] Falcão D.S., Gomes P.J., Oliveira V.B., Pinho C., Pinto A.M.F.R., 1D and 3D numerical simulations in PEM fuel cells, *International Journal of Hydrogen Energy*, September 2011, 36 (19): 12486-12498.
- [14] Sarmiento-Carnevali M., Serra M., Batlle C., Distributed parameter model simulation tool for PEM fuel cells, *International Journal of Hydrogen Energy*, March 2014, 39 (8): 4044-4052.